Frenkel exciton model of ultrafast excited state dynamics in AT DNA double helices

Eric R. Bittner[*]

Department of Chemistry and the Texas Center for Superconductivity,
University of Houston, Houston, TX 77204, United States

Abstract

Recent ultrafast experiments have implicated intrachain base-stacking rather than base-pairing as the crucial factor in determining the fate and transport of photoexcited species in DNA chains. An important issue that has emerged concerns whether or not a Frenkel excitons is sufficient one needs charge-transfer states to fully account for the dynamics. Here we present an $SU(2) \otimes SU(2)$ lattice model which incorporates both intrachain and interchain electronic interactions to study the quantum mechanical evolution of an initial excitonic state placed on either the adenosine or thymidine side of a model B DNA poly(dA).poly(dT) duplex. Our calculations indicate that over several hundred femtoseconds, the adenosine exciton remains a cohesive excitonic wave packet on the adenosine side of the chain where as the thymidine exciton rapidly decomposes into mobile electron/hole pairs along the thymidine side of the chain. In both cases, the very little transfer to the other chain is seen over the time-scale of our calculations. We attribute the difference in these dynamics to the roughly 4:1 ratio of hole versus electron mobility along the thymidine chain. We also show that this difference is robust even when structural fluctuations are introduced in the form of static off-diagonal disorder.

© 2006 Elsevier B.V. All rights reserved.

PACS: 87.14.Gg; 87.15.Mi; 87.15.He; 31.15.Ar

Keywords: DNA; Molecular biophysics; Excited states; Lattice theory; Quantum chromodynamics

1. Introduction

For all life-forms on Earth with the exception of certain viruses, genetic information is carried within the cellular nucleus via strands of strands of deoxyribonucleic acid (DNA). The genetic information itself is encoded in the specific sequence of the nucleic acid bases: adenine (A), thymine (T), guanine (G), and cytidine (C). DNA is also a strong absorber of ultraviolet light leaving it highly susceptible to photomutagenic damage with the primary photoproducts being bipyrimidine dimers linking neighboring T bases. For all organisms, this susceptibility is compensated for in part through enzymatic repair actions that remove damaged segments along one strand using the complementary strand as a template for replacement. Such repair mechanisms are quite costly energetically. Remarkably, how-

ever, DNA is intrinsically photochemically stable as single bases are able to rapidly convert photoexcitation energy into thermal energy on a picosecond time scale through non-radiative electronic processes. What remains poorly understood is the role that base-pairing and base-stacking plays in the transport and migration of the initial excitation along the double helix. Clearly, such factors are important since the UV absorption of DNA largely represents the weighted sum of the absorption spectra of it constituent bases whereas the distribution of lesions formed as the result of photoexcitation are generally not uniformly distributed along the chain itself and depend strongly upon sequence, suggesting some degree of coupling between bases [1].

Given the importance of DNA in biological system and its emerging role as a scaffold and conduit for electronic transport in molecular electronic devices [2], DNA in its many forms is a well-studied and well-characterized system. What remains poorly understood, however, is the role that base-pairing and base-stacking plays in the transport and migration of the initial excitation along the double helix [3,1]. Such factors are

* Tel.: +1 713 743 2775; fax: +1 713 743 2709.
  E-mail address: bittner@uh.edu.

important since the UV absorption of DNA largely represents the weighted sum of the absorption spectra of it constituent bases whereas the distribution of lesions formed as the result of photoexcitation are generally not uniformly distributed along the chain itself and depend strongly upon sequence, suggesting some degree of coupling between bases [1].

Recent work by various groups has underscored the different roles that base-stacking and base-pairing play in mediating the fate of an electronic excitation in DNA [1,3]. Over 40 years ago, Lowdin discussed proton tunneling between bases as a excited state deactivation mechanism in DNA [4] and evidence of this was recently reported by Schultz et al. [5]. In contrast, however, ultrafast fluorescence of double helix poly(dA).poly(dT) oligomers by Crespo-Hernandez et al. [3] and by Markovitsi et al. [1] give compelling evidence that base-stacking rather than base-pairing largely determines the fate of an excited state in DNA chains composed of A and T bases with long-lived intrastrand states forming when ever A is stacked with itself or with T. However, there is considerable debate regarding whether or not the dynamics can be explained via purely Frenkel exciton models [6–8] or whether charge-transfer states play an intermediate role [9].

Here we report on a series of quantum dynamical calculations that explore the fate of a localized exciton placed on either the A side or T side of the B DNA duplex poly(dA)$_{10}$.poly(dT)$_{10}$. Our theoretical model is based upon a $SU(2) \otimes SU(2)$ lattice model we recently introduced [10] that consists of localized hopping interactions for electrons and holes between adjacent base pairs along each strand (t_{aj}) as well as cross-strand terms linking paired bases (h_i) and "diagonal" terms which account for the π-stacking interaction between base j on one chain and base $j \pm 1$ on the other chain ($r_i^{\pm}$) in which r_j^- denotes coupling in the 5′-5′ direction and r_i^+ coupling in the 3′-3′ direction. Fig. 1 shows the three-dimensional structure of poly(dA)$_{10}$.poly(dT)$_{10}$ and the topology of the equivalent lattice model. We also consider here the role of geometric or structural fluctuations in the electronic dynamics.

2. Theoretical model

Taking each link as Fig. 1 as a specific electron, hole, or excitonic, hopping term, we arrive at the following single particle Hamiltonian,

$$h_1 = \sum_j \epsilon_j \hat{\psi}_j^\dagger \hat{\psi}_j + t_j(\hat{\psi}_{j+1}^\dagger \hat{\psi}_j + \hat{\psi}_j^\dagger \hat{\psi}_{j+1}) + h_j \bar{\psi}_j \hat{\psi}_j$$
$$+ \hat{\psi}_{j+1}^\dagger(r_j^+ \hat{\gamma}_+ + r_j^- \hat{\gamma}_-)\hat{\psi}_j + \hat{\psi}_j^\dagger(r_j^+ \hat{\gamma}_+ + r_j^- \hat{\gamma}_-)\hat{\psi}_{j+1}$$

$$(1)$$

where $\hat{\psi}_j^\dagger$ and $\hat{\psi}_j$ are $SU(2)$ spinors that act on the ground-state to create and remove an electron (or hole) on the jth adenosine or thymidine base along the chain. The $\hat{\gamma}$ operators are the 2×2 Pauli spin matrices with $\bar{\psi}_j = \hat{\gamma}_1 \hat{\psi}_j^\dagger$ and $\hat{\gamma}_+ + \hat{\gamma}_- = \hat{\gamma}_1$ providing the mixing between the two chains. As discussed in Ref. [10], we used the highest occupied and lowest unoccupied (π and π^*) orbitals localized on each base as a orthonormal basis. For the single particle terms (representing electron and hole transfer between bases), we use values reported by Mehrez and Anantram as determined by computing the Coulomb integrals between HOMO and LUMO levels on adjacent base pairs with in a double-strand B DNA sequence using density functional theory (B3LYP/6-31G) [11] taking the geometries of each base from the B-DNA structure. When $r_j^+ = r_j^-$, Eq. (2) is identical to the Hamiltonian used by Creutz and Horvgath [12] to describe chiral symmetry in quantum chromodynamics in which the terms proportional to r are introduced to make the "doublers" at $q \propto \pi$ heavier than the states at $q \propto 0$.

Taking the chain to homogeneous and infinite in extent, one can easily determine the energy spectrum of the valence and conduction bands by diagonal-izing

$$\hat{h}_1 = \begin{pmatrix} \epsilon_a + 2t_a \cos(q) & h + r^+ e^{-iq} + r^- e^{+iq} \\ h + r^+ e^{+iq} + r^- e^{-iq} & \epsilon_b + 2t_b \cos(q) \end{pmatrix} \quad (2)$$

where $\epsilon_{a,b}$, and $t_{a,b}$ are the valence band or conduction band site energies and intra-strand hopping integrals. When $r_j^+ = r_j^-$, Eq. (2) is identical to the Hamiltonian used by Creutz and Horvgath [12] to describe chiral symmetry in quantum chromodynamics in which the terms proportional to r are introduced to make the "doublers" at $q \propto \pi$ heavier than the states at $q \propto 0$. In particular, we note that when $t = h/2r$, the band closes at $q = \pm \pi$ but has a gap at $q = 0$.

The single particle parameters are taken from Mehrez and Anantram as determined by computing the Coulomb integrals between HOMO and LUMO levels on adjacent base pairs with in a double-strand B DNA sequence using density functional
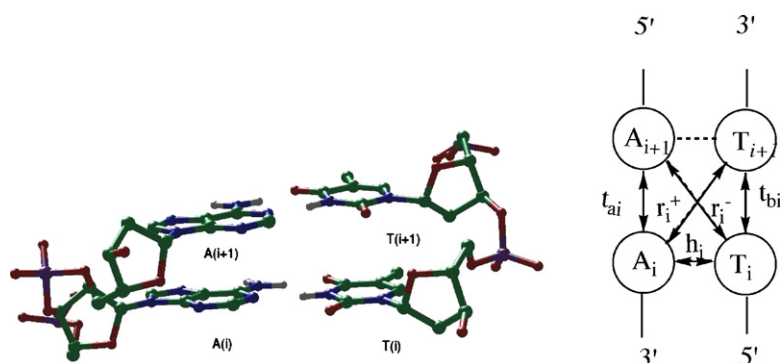

Fig. 1. Three-dimensional structure of stacked A–T base pairs along with the corresponding lattice model.

Table 1
Charge-transfer and exciton transfer terms for AT DNA. (B-FORM)

Description	Value	References
Intrachain e transfer: $A_i - A_{i+1}$	$t_{ea} = +0.024$ eV	[11]
Intrachain e transfer: $T_i - T_{i+1}$	$t_{eb} = -0.023$ eV	[11]
Interchain e transfer: $A_i - T_i$	$h_e = +0.063$ eV	[11]
Interchain 3'-3' e transfer: $A_i - T_{i+1}$	$r_i^+ = -0.012$ eV	[11]
Interchain 5'-5' e transfer: $A_i - T_{i+1}$	$r_i^- = -0.016$ eV	[11]
Intrachain h transfer: $T_i - T_{i+1}$	$t_{hb} = -0.098$ eV	[11]
Intrachain h transfer: $A_i - A_{i+1}$	$t_{ha} = +0.021$ eV	[11]
Interchain h transfer: $A_i - T_{i-1}$	$h_h = +0.002$ eV	[11]
Interchain 3'-3' h transfer: $A_i - T_{i+1}$	$r_i^+ = -0.007$ eV	[11]
Interchain 5'-5' h transfer: $A_i - T_{i-1}$	$r_i^- = +0.050$ eV	[11]
Intrachain parallel dipole-dipole: $T_i - T_{i+1}$	$d_\parallel^T = 0.143$ eV	[10]
Intrachain parallel dipole-dipole: $A_i - A_{i+1}$	$d_\parallel^A = 0.0698$ eV	[10]
Interchain perpendicular dipole–dipole: $A_i - T_i$	$d_\perp = -0.099$	[10]
Interchain 3'-3' dipole–dipole: $A_i - T_{i+1}$	$d^+ = -0.013$ eV	[10]
Interchain 5'-5' dipole–dipole: $A_i - T_{i-1}$	$d^- = -0.006$ eV	[10]
Site energies		
A(LUMO)	$\epsilon_{Ae} = 0.259$ eV	[11]
A(HOMO)	$\epsilon_{Ah} = -5.45$ eV	[11]
T(LUMO)	$\epsilon_{Te} = -0.931$ eV	[11]
T(HOMO)	$\epsilon_{Th} = -6.298$ eV	[11]

theory (B3LYP/6-31G) [11]. Parameters used in our model are presented in Table 1. It is important to note that the asymmetry introduced with $r_j^+ \neq r_j^-$ gives directionality between the 3'- and 5'-ends of the chain. Introducing these parameters into Eq. (2) leads to four separate cosine shaped bands corresponding to conduction and valence bands localized along each chain as show in Fig. 2.

The coupling between the conduction and valence bands is accomplished by introducing short-ranged Coulomb and exchange interactions as well as "dipole-dipole" terms which couple geminate electron-hole pairs on different sites and considering only single excitations,

$$H(12) = h_1 + h_2 + \sum_{m,n} V_{m,n} A_m^\dagger A_n \qquad (3)$$

where the A_m are spin-symmetrized composite operators that create or remove singlet or triplet electron/hole pairs in configuration $|m\rangle = |i\bar{j}\rangle$ where $V_{mn} = -\langle m\bar{n}||n\bar{m}\rangle + 2\delta_{S0}\langle m\bar{n}||\bar{n}m\rangle$ where $S = 1,0$ is the total spin. [13–16] In our model, we include three types of electron/hole interactions, an on-site direct Coulomb $J = \langle n\bar{n}||n\bar{n}\rangle$, an on-site exchange term $K = \langle n\bar{n}|\bar{n}n\rangle$, and an inter-site singlet exciton transfer term: $d_{mn} = \delta_{S0}\langle m\bar{m}||n\bar{n}\rangle$.

For simplicity, we take the on-site Coulomb interaction as $J = \langle n\bar{n}||n\bar{n}\rangle$ and the on-site exchange interaction $K = \langle n\bar{n}|\bar{n}n\rangle$ to be adjustable parameters with values $J = 2.5$ eV and $K = 1.0$ eV for both purines and pyrimidines. We assume these interactions to be local since the distance at which the Coulomb energy between an electron/hole pair equals the thermal energy in aqueous ionic media at 300 K is on the order of the base-stacking
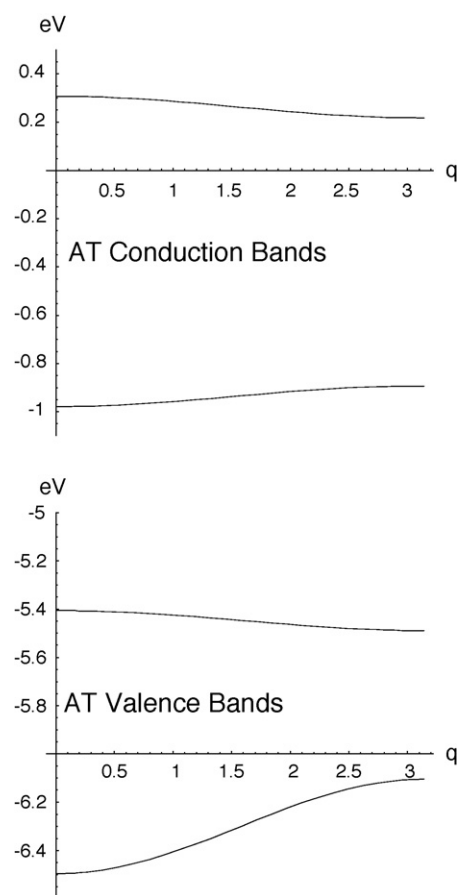

Fig. 2. (L) Band structure for homogeneous AT DNA chain.

distance. Furthermore, such values are certainly in the correct range for conjugated cyclic organic systems. [13–16] Lastly, we estimated the coupling between geminate electron/hole pairs on different bases $\langle n\bar{n}||m\bar{m}\rangle$ via a point-dipole approximation by mapping the $\pi - \pi^*$ transition moments onto the corresponding base in the B DNA chain. These are obtained from the isolated bases by performing single configuration interaction (CIS) calculations using the GAMESS [17] quantum chemistry package on the corresponding 9-methylated purines and 1-methylated pyrimidines after optimizing the geometry at the HF/6-31(d)G level of theory.

The use of the point-dipole approximation in this case is justified mostly for convenience and given the close proximity of the bases, multipole terms should be included in a more complete model. [18] As a result, the matrix elements used herein provide an upper limit (in magnitude) of the couplings between geminate electron-hole pairs. Most importantly, however, the point-dipole approximation provides a robust means of incorporating the geometric arrangement of the bases into our model [10].

3. Excited state dynamics: homogeneous lattice

We now consider the fate of an initial singlet electron/hole pair placed either in the middle of the thymidine side of the chain or the adenosine side of the chain (i.e. a localized exciton with

the electron and hole starting on the same site). We assume that such a configuration is the result of an photoexcitation at the appropriate photon energy (4.87 eV for the thymidine exciton and 5.21 eV for the adenosine exciton respectively) and based upon the observation that the UV absorption spectra largely represents the weighted sum of the UV spectra of the constituent bases. Since these are not stationary states, they evolve according to the time-dependent Schrödinger equation, which we integrate using the Tchebychev expansion of the time-evolution operator [19].

In the top two frames of Fig. 3 we show the transient probability for finding an exciton placed on the adenosine (left) or thymidine (right) chain at time $t = 0$ in some other excitonic configuration along either the adenosine or thymidine chain at some time t later. In both cases, negligible exciton density is transferred between chains and the excitons rapidly become delocalized and scatter ballistically down the DNA chain.

There are some striking differences, however, between the exciton dynamics in adenosine versus those in thymidine. First, in comparing the $d_{||}$ matrix elements, one easily concludes that the exciton mobility along the thymidine chain is considerably greater than the mobility along the adenosine chain. This can be see in Fig. 2. comparing the time required for an excitonic wavepacket to reach the end of either chain. In adenosine, the exciton travels nearly 5 base pairs in about 25 fs where as an

exciton along the thymidine chain covers the same distance in about 10 fs. This factor of two difference in the exciton velocity is commensurate with the $\approx$1:2 ratio of the $d_\perp^A : d_\perp^T$ intrachain excitonic couplings.

Secondly, we note that the adenosine exciton remains qualitatively more "cohesive" than the thymidine exciton showing a number of ballistic traverses up and down the adenosine chain over the 300 fs we performed the calculation. One can also note that the exciton velocity in the $5'$-$3'$ direction is slightly greater than in the $3'$-$5'$ direction as evidenced by the exciton rebounds off site A_1 slightly sooner than it rebounds from site A_{10}. This is due to the asymmetry introduced in by the $r^\pm$ and $d^\pm$ terms. All in all, one can clearly note a series of strong recurrences for finding the adenosine exciton on the original site A_5 every 100 fs. The thymidine exciton dynamics are far more complex as the exciton rapidly breaks apart. While few recursions can be noted, however, after the first ballistic traverse, the thymidine exciton no longer exists as a cohesive wavepacket and is more or less uniformly distributed along the thymidine side of the chain.

The excitonic dynamics only tell part of story. In the lower frames of Fig. 3 we show the net charge taken as the difference between the hole density and electron density on a given base. In the case where the initial exciton is on the adenosine chain, very little charge-separation occurs over the time scale of our calculation. On the other hand, when the exciton is placed on
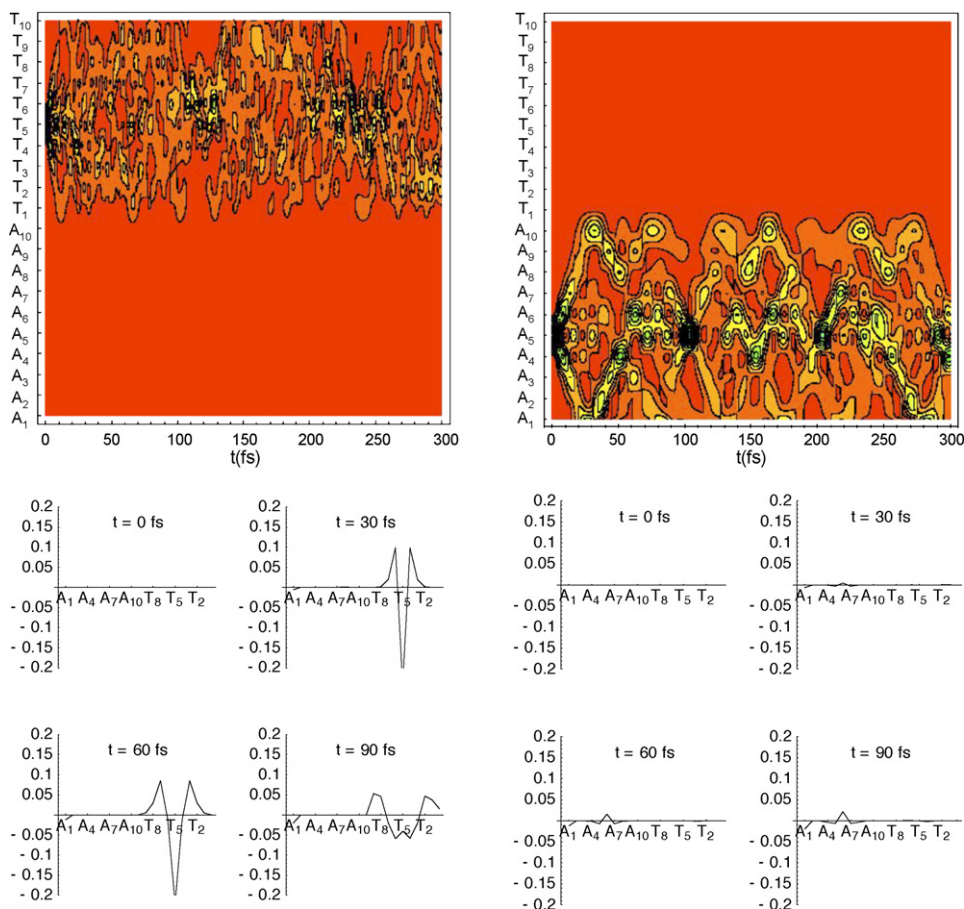

Fig. 3. Time evolution of excitonic density following excitation placed on T_5 (top-left) or A_5 (top-right) site. The bottom panels show the net charge on each site following excitation of T_5 (bottom-left) or A_5 (bottom-right).
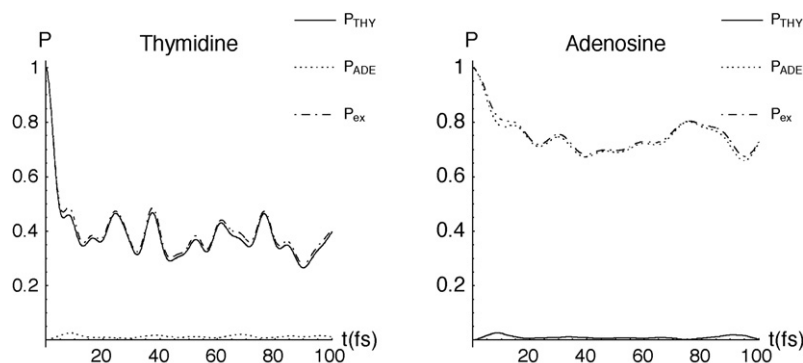
Fig. 4. Net probability for an exciton originating on the thymidine (left) or adenosine (right) side of the chain to remain as an exciton on the original chain, to be found as an exciton on the other chain, and total exciton population.

the thymidine chain, the exciton almost *immediately* evolves into a linear combination of excitonic and charge-separated configurations. What is also striking is that in neither case do either the electron or hole transfer over to the other chain even though energetically charge-separated states with the electron on the thymidine and the hole on the adenosine sides of the chain are the lowest energy states of our model. [10] It is possible, that by including dissipation or decoherence into our dynamics, such relaxation will occur, however, on a time scale dictated by cross-chain transfer terms. For the coupling terms at hand, electron or hole transfer across base pairs occurs on the time scale of 3–4 ps.

The difference between the excitonic dynamics following excitation of A versus T can be quantitatively noted by comparing the curves shown in Fig. 4 where we compare the projection of the time-evolved state onto the excitonic configurations of the chain on which the exciton was placed (P_{AA} and P_{TT}) compared to the projection onto the excitonic configurations of the other chain (P_{AT} and P_{TA}). For the case in which the adenosine chain was excited, approximately 75% of the total probability density remains as excitonic configurations along the adenosine chain. In stark contrast, only about 40% of the initial thymidine exciton remains excitonic along the thymidine side of the chain. The reason for the remarkable difference between the two chains stems from the difference in electron and hole mobility along the thymidine chain. Indeed, comparing the electron and hole hopping terms given above, $t_h/t_e \approx 4$ for the thymidine chain compared to $t_h/t_e \approx 1$ for along the adenosine chain. This is manifest in the lower left panel of Fig. 3 where we see almost immediately a negative charge remaining for a few fs on the site where the initial excitation was placed. In contrast, no charge-separation is seen following excitation along the adenosine side of the chain.

4. Excited state dynamics: effects of static disorder

A proper model of the electronic dynamics in DNA must include some contribution from the solvent and environment. For DNA in water at 300 K, we assume that the electronic processes described in our model are fast compared to the structural and environmental fluctuations the DNA lattice itself such that the parameters for the B-DNA structure represent the average values for the system in aqueous media. For example, the characteristic

time scale for the relative lateral and longitudinal motions of bases in DNA is 10–100 fs with amplitudes of 0.01–0.1 nm. [20] Since electronic interactions between bases are sensitive to the fluctuations in the geometry of the DNA structure, factors such as salt concentration and other solvent media will have profound impact on the structure and hence on the model parameters.

Since short strands of DNA are fairly rigid, the electronic coupling terms are likely most sensitive upon the dihedral angle, θ_{ij} between adjacent bases. If we take the fluctuations in θ_{ij} to be $\delta\theta^2 = K_B T/I\Omega^2$ where I is the reduced moment of inertia of the AT base-pair and $\Omega = 25\,\text{cm}^{-1}$ is the torsional frequency. This gives an RMS angular fluctuation of about 5% about the avg. $\overline{\theta_{i,i+1}} = 35.4°$ helical angle. Since this is a small angular deviation, we take the fluctuations in the electronic terms to be proportional to $\delta\theta^2$ and sample these terms from normal distributions about B-DNA average values.

The effect of disorder on the excitonic dynamics are seen in Fig. 5. As in case of the homogeneous lattice above, our initial state is a Frenkel exciton on thymidine #5. The right-hand plot of Fig. 5 shows the probability of finding the time-evolved state in various excitonic configurations. While the time-scale for the exciton break up is slower than in the homogenous lattice, one can deduce that even with static off-diagonal disorder, the thymidine exciton is subject to dissociate to charge-transfer (i.e. polaron) pairs on an ultrafast timescale. The adenosine exciton appears to be more profoundly affected by the lattice disorder with some population transfered to the thymidine chain. Since the total exciton population is lowered upon introducing disorder, the remaining excited state population exists as charge-separated pairs. Analysis of the transient excited state wavepackets (not-shown) indicates a small but significant fraction of $A_i^+ - T_i^-$ interstrand charge-transfer configurations.

Lastly, we examine the relative mobilities of the electron and hole by calculating the RMS width of the electron and hole densities on either chain following excitation, the results of which are shown in Fig. 6. In the top two plots are the RMS widths for the homogeneous lattice following excitation. As discussed above, the hole is considerably more mobile than the electron along the thymidine side of the chain. This is very much evidenced by the more rapid spread of the hole density compared to the electron density. Likewise, along the adenosine side, the conduction and valence bands have nearly identical band-widths
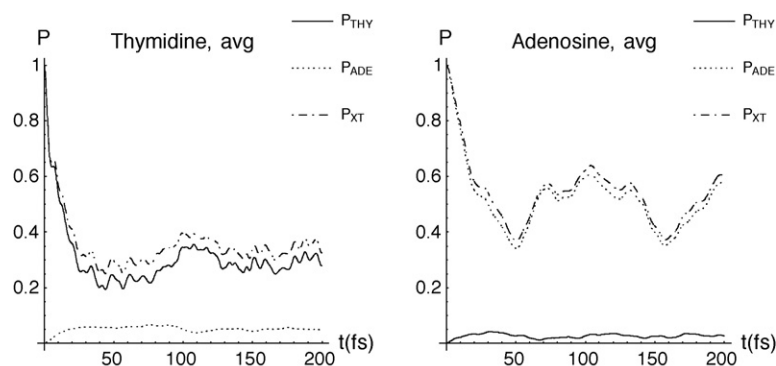
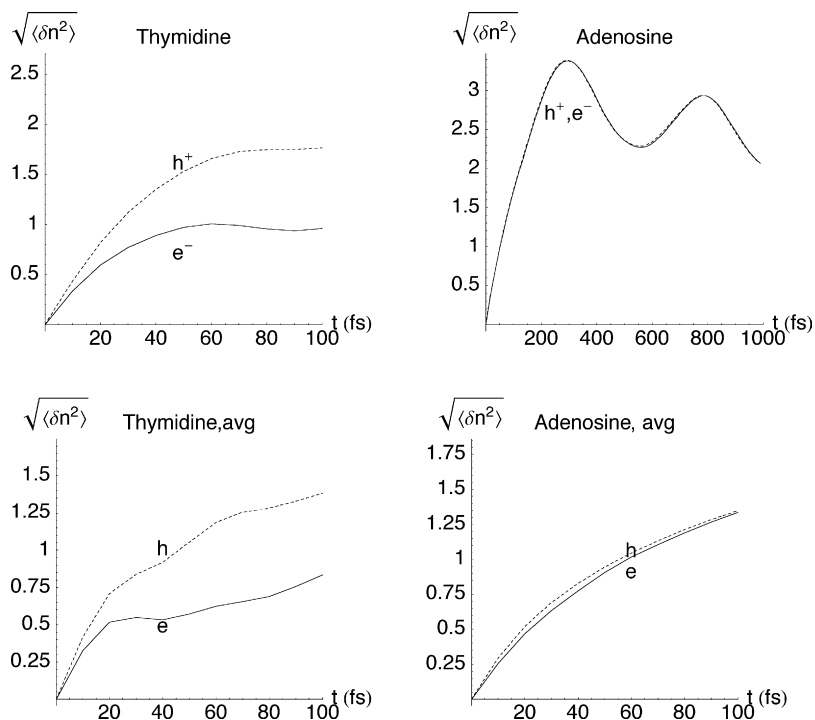Fig. 5. Same as in Fig. 4 except averaging over ensemble of configurations.

Fig. 6. RMS width of electron and hole densities vs. time for excitations originating on different sides of the AT chain: Top, homogeneous chain; Bottom, averaging over 20 random lattice configurations.

and the electron and hole densities evolve very much in concert. This scenario is preserved even upon averaging over configurations indicating that within a 5% error in our parameter set or within the typical thermal fluctuations of a DNA chain, our predicted dynamics are quite robust.

5. Summary

The results described herein paint a similar picture to that described by recent ultrafast spectroscopic investigations of (dA).(dT) oligomers in that the initial excitonic dynamics is dominated by base-stacking type interactions rather than by inter-base couplings. Interchain transfer is multiple orders of magnitude slower than the intrachain transport of both geminate electron/hole pairs as excitons and independent charge-separated species. Indeed, for an exciton placed on the adenosine chain, our model predicts that exciton remains as a

largely cohesive and geminate electron/hole pair wave function as it scatters along the adenosine side of the chain. Our model also highlights how the difference between the mobilities in the conduction and valence bands localized along each chain impact the excitonic dynamics by facilitating the break up of the thymidine exciton into separate mobile charge-carriers. In the actual physical system, the mobility of the free electron and hole along the chain will certainly be dressed by the polarization of the medium and reorganization of the lattice such that the coherent transport depicted here will be replaced by incoherent hopping between bases.

The significance of the breakup of the exciton is twofold. First, it is well recognized that photoexcitation of adjacent stacked pyrimidine bases leads to the formation of *cis-syn* cyclobutane pyrimidine-dimer lesions. However, this dimerization occurs only in the triplet (rather than singlet) excited state. [21] Consequently, spin-flip must occur *ether* via spin-orbit cou-

pling or via recombination of polaron pairs. [16] If we assume that the spins are decorrelated at some intermediate distance $r \propto e^2/\epsilon kT$, where the Coulomb energy is equal to the thermal energy, photoexcitation of a thymine sequence could rapidly result in a population of triplet excitons formed by exciton dissociation followed by geminate recombination. Secondly, the process is reversible and triplet reactivation of the dimer can lead to repair of the lesion.

Isolating the photoexcitation to the originally excited chain minimizes the potential mutagenic damage to the DNA sequence since it preserves the complementary chain as an undamaged back-up copy of the genetic information. It is fascinating to speculate whether or not the isolation of a photoexcitation and its photoproducts to the original chain was an early evolutionary selection criteria for the eventual emergence of DNA as the carrier of genetic information.

In conclusion, we present herein a rather compelling model for the short-time dynamics of the excited states in DNA chains that incorporates both charge-transfer and excitonic transfer. It is certainly not a complete model and parametric refinements are warranted before quantitative predictions can be established. For certain, there are various potentially important contributions we have left out: disorder in the system, the fluctuations and vibrations of the lattice, polarization of the media, dissipation, quantum decoherence. We hope that this work serves as a starting point for including these physical interactions into a more comprehensive description of this system.

Acknowledgments

References

[1] D. Markovitsi, D. Onidas, T. Gustavsson, F. Talbot, E. Lazzarotto, Collective behavior of Franck-Condon excited states and energy transfer in DNA double helices, J. Am. Chem. Soc. 127 (2005) 17130–17131.

[2] S.O. Kelley, J. K. Barton, Electron transfer between bases in double helical DNA, Science 283 (1999) 375. URL http://www.sciencemag.org/cgi/content/abstract/283/5400/375.

[3] C.E. Crespo-Hernandez, B. Cohen, B. Kohler, Base stacking controls excited state dynamics in A-T DNA, Nature 436 (2005) 1141.

[4] P.O. Lowin, Proton tunneling in DNA and its biological implications, Rev. Mod. Phys. 35 (1963) 724.

[5] T. Schultz, E. Samoylova, W. Radloff, V.H. Ingolf, A.L. Sobolewski, W. Domcke, Efficient deactivation of a model base pair via excited-state hydrogen transfer, Science 306 (2004) 1765-8. URL http://www.sciencemag.org/cgi/content/abstract/306/5702/1765.

[6] E. Emanuele, D. Markovitsi, P. Millie, K. Zakrzewska, UV spectra and excitation delocalization in DNA: influence of the spectral width, ChemPhysChem 6 (2005) 1387–1393.

[7] E. Emanuele, K. Zakrzewska, D. Markovitsi, R. Lavery, P. Millie, Exciton states of dynamic DNA double helices: alternating dCdG sequences, J. Phys. Chem. B 109 (2005) 16109–16118.

[8] D. Markovitsi, F. Talbot, T. Gustavsson, D. Onidas, E. Lazzarotto, S. Marguet, Molecular spectroscopy: complexity of excited-state dynamics in DNA, Nature 441 (2006) E7, URL http://www.nature.com/nature/journal/v441/n7094/pdf/nature04903.pdf.

[9] C.E. Crespo-Hernandez, B. Cohen, B. Kohler, Molecular spectroscopy: complexity of excited-state dynamics in DNA (reply), Nature 441 (2006) E8, URL http://www.nature.com/nature/journal/v441/n7094/pdf/nature04904.pdf.

[10] E.R. Bittner, Lattice theory of ultrafast excitonic and charge-transfer dynamics in DNA, J. Chem. Phys. 125 (9) (2006) 094909, URL http://link.aip.org/link/?JCP/125/094909/1.

[11] H. Mehrez, M.P. Anantram, Interbase coupling for transport through DNA, Phys. Rev. B 71 (2005) 115405, URL http://link.aps.org/abstract/PRB/v71/e115405.

[12] M. Creutz, I. Horvgath, Surface modes and chiral symmetry (Wilson Fermions in a box), Nucl. Phys. B (Proc. Supp.) 34 (1994) 583.

[13] S. Karabunarliev, E.R. Bittner, Polaron-excitons and electron-vibrational band shapes in conjugated polymers, J. Chem. Phys. 118 (9) (2003) 4291–4296, URL http://link.aip.org/link/?JCP/118/4291/1.

[14] S. Karabunarliev, E.R. Bittner, Dissipative dynamics of spin-dependent electron-hole capture in conjugated polymers, J. Chem. Phys. 119 (7) (2003) 3988–3995, URL http://link.aip.org/link/?JCP/119/3988/1.

[15] S. Karabunarliev, E.R. Bittner, Electroluminescence yield in donor-acceptor copolymers and diblock polymers: a comparative theoretical study, J. Chem. Phys. 108 (29) (2004) 10219–10225.

[16] S. Karabunarliev, E.R. Bittner, Spin-dependent electron-hole capture kinetics in luminescent conjugated polymers, Phys. Rev. Lett. 90 (5) (2003) 057402, URL http://link.aps.org/abstract/PRL/v90/e057402.

[17] M.W. Schmidt, K.K. Baldridge, J.A. Boatz, S.T. Elbert, M.S. Gordon, J.H. Jensen, S. Koseki, N. Matsunaga, K.A. Nguyen, S.J. Su, T.L. Windus, M. Dupuis, J.A. Montgomery, General atomic and molecular electronic structure system, J. Comput. Chem. 14 (1993) 1347.

[18] B. Bouvier, T. Gustavsson, D. Markovitsi, P. Millie, Dipolar coupling between electronic transitions of the DNA bases and its relevance to exciton states in double helices, Chem. Phys. 275 (2002) 75–92.

[19] H. Tal-Ezer, R. Kosloff, An accurate and efficient scheme for propagating the time dependent Schrödinger equation, J. Chem. Phys. 81 (9) (1984) 3967–3971, URL http://link.aip.org/link/?JCP/81/3967/1.

[20] J.A. McCammon, S.C. Harvey, Dynamics of Proteins and Nucleic Acids, second ed., Cambridge University Press, Cambridge, 1987.

[21] R.P. Sinha, D.-P. Hadler, UV-induced DNA damage and repair: a review, Photochem. Photobiol. Sci. 1 (2002) 225–236, URL doi:10.1039/b201230h.